The Metabolite Ratio in Spectroscopic Imaging of Prostate Cancer

Alan J. Wright; Thiele Kobus; Arend Heerschap; Tom W. J. Scheenen

Radboud University Nijmegen Medical Centre, Radiology Department, Nijmegen, The Netherlands

Introduction

Prostate cancer is the second leading cause of cancer related death in Western countries [1]. The prevalence of the disease is very high, but many men diagnosed with the disease will die from unrelated causes. This is because prostate cancer very often is a disease of old age that grows slowly. Common treatment for prostate cancer in clinical practice involves radical resection of the entire gland or radiotherapy with a dose distributed over the whole organ. Provided that the cancer has not metastasized, these therapies are curative, though concern over their side effects has led to patients and their doctors delaying this treatment and, instead, entering into active surveillance or watchful waiting programs. In order for patients to safely forgo curative treatment, it is essential to characterize their disease: to determine that it is sufficiently benign that growth will be slow and metastasis improbable. Selecting these patients, with low risk disease, that are appropriate for active surveillance requires accurate diagnosis of not just the presence of tumor, but how aggressive it is: i.e. how fast it is growing and how likely it is to metastasise to the lymphatic system. Magnetic resonance imaging (MRI) is an emerging technique for making this patient selection. It can diagnose the presence of tumor, localize it in the organ and provide information as to how aggressive it is. The MRI exams employed for this purpose usually involve multiple imaging sequences including a T2-weighted sequence, diffusion-weighted imaging (DWI) and one or more further techniques such as dynamic contrast enhanced MRI (DCE-MRI) or Proton Magnetic Resonance Spectroscopic Imaging (^{1}H MRSI) [2].

Radiologists can read the different imaging modalities to decide the location, size and potential malignancy of the tumor which are all indicators of its metastatic potential. Acquiring and reporting imaging data in this way is known as multiparametric (mp) MRI. MRSI is the only mpMRI methodology that acquires data from molecules other than water [19]. A three dimensional (3D) ^{1}H MRSI data set consists of a grid of spatial locations throughout the prostate (see Fig. 1) called voxels. For each voxel a spectrum is available. Each spectrum consists of a number of peaks on a frequency axis, corresponding to resonances from protons with a certain chemical shift in different molecules. The size of a peak at a certain frequency (chemical shift) corresponds to the amount of the metabolite present in the voxel. In this way MRSI measures the bio-chemicals in regions of tissue *in vivo* without the need for any external contrast agent or invasive procedures. Examples of spectra from two voxels, acquired at a magnetic field strength of 3 Tesla (3T), are given in figure 1B, C, which clearly shows the differing profiles that are characteristic of benign prostate tissue and its tumors.

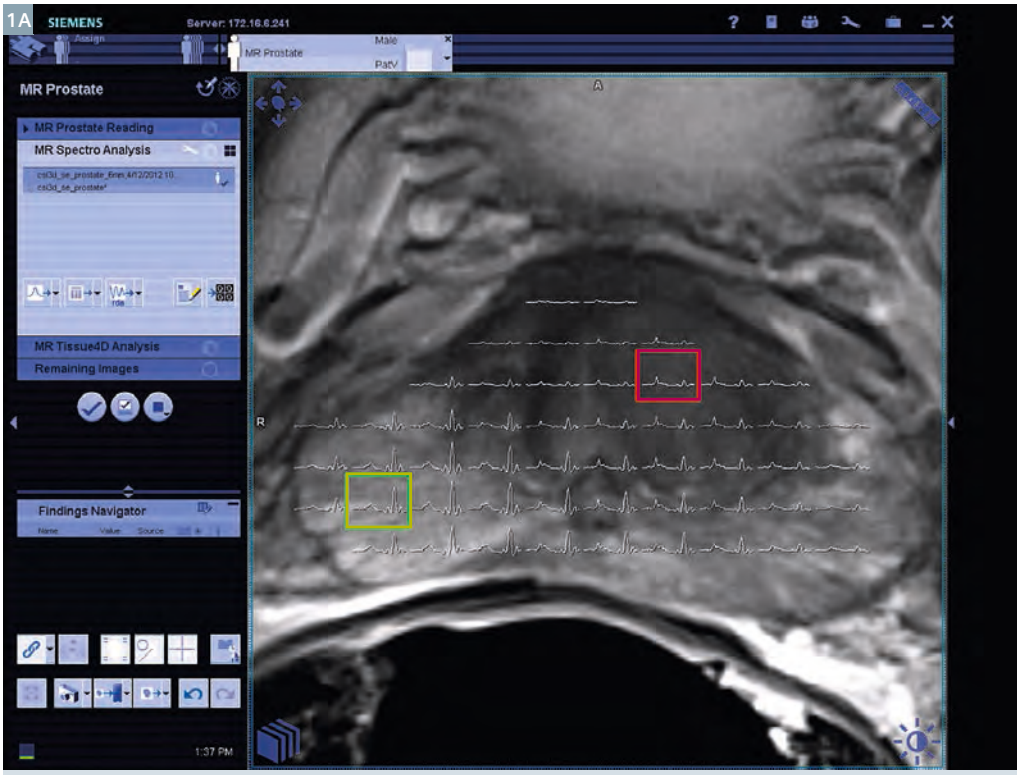

1 **(1A)** T2-weighted MR image of a transverse section through a prostate with an overlaid grid of MRSI spectra from voxels within the prostate.

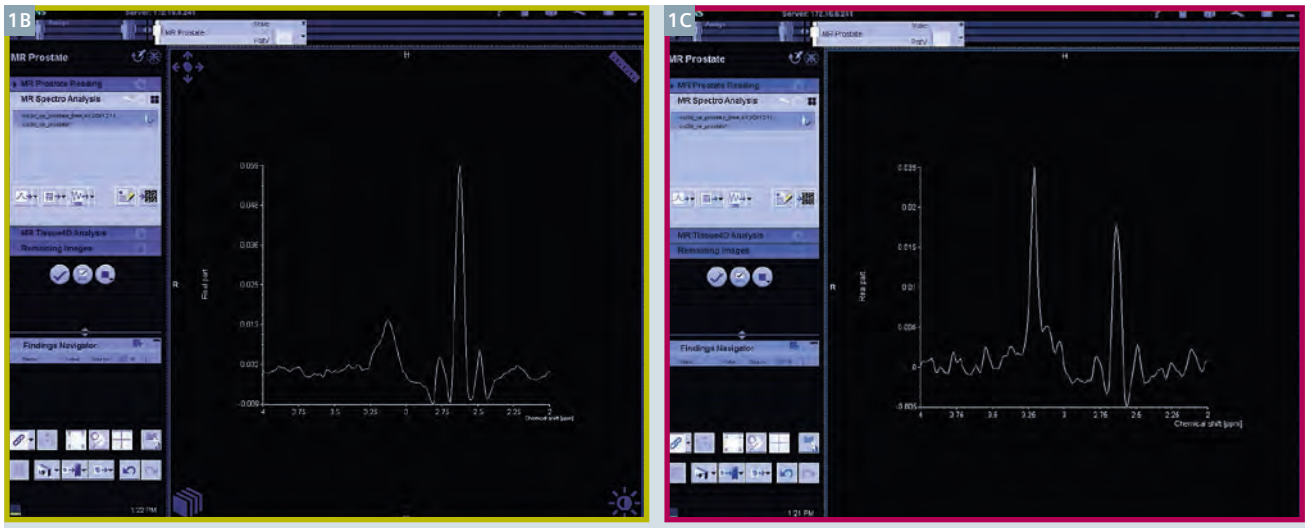

1 **(1B)** One example spectrum shown on a ppm scale from a region of benign prostate tissue. **(1C)** A spectrum from another voxel that, in this case, co-localises to a region of tumor.

Important metabolites in prostate MRSI

The initial papers on *in vivo* prostate MRSI were performed at a magnetic field strength of 1.5T [3-5], and three assignments were provided for the observed resonances: choline, creatine and citrate (Fig. 2). The small number of these assignments reflected the simplicity of the spectrum, which contained two groups of resonances: one in the region of 3.3 to 3 ppm, which will be referred to as the choline-creatine region, and another at 2.55–2.75 ppm, which shall be called the citrate group. These assignments related to what were believed to be the strongest metabolite resonances. People should be aware however, that the assignments are representative of multiple similar molecules. The choline assignment reflects the methyl resonances from multiple compounds containing a choline group (Fig. 4): choline, phosphocholine and glycerophosphocholine. Similarly, creatine refers to both creatine and phosphocreatine. In between the choline and creatine signals another group of resonances are present: the polyamines (mainly spermine and spermidine). The citrate resonances are from citrate only but can have a complicated shape, although *in vivo* at 1.5T they give the appearance of a single peak. Nowadays a magnetic field strength of 3T is used more and more for prostate spectroscopic imaging, which gives opportunities to better resolve the choline, polyamines, creatine resonances, but also changes the shape of the citrate signal.

Larger choline signals are associated with tumor in nearly all cancers [6]. High choline signals are interpreted as being evidence of rapid proliferative growth and, more directly, the increased membrane turnover required for cell division. Membranes contain phospholipids: phosphatidyl choline and phosphatidyl ethanolamine, which are synthesised by a metabolic pathway involving choline-containing metabolites known as the Kennedy pathway. It is in the synthesis and catabolism of these products, upregulated in proliferative tumor growth, that causes the increase in these signals.

The large amplitude of citrate resonances observed in prostate tissue is due to an altered metabolism particular to this gland. Prostate tissue accumulates high concentrations of zinc ions which inhibit mitochondrial aconitase, leading to a build up of citrate in the prostate's epithelial cells [7]. This citrate is further secreted into the ductal spaces of the prostate as

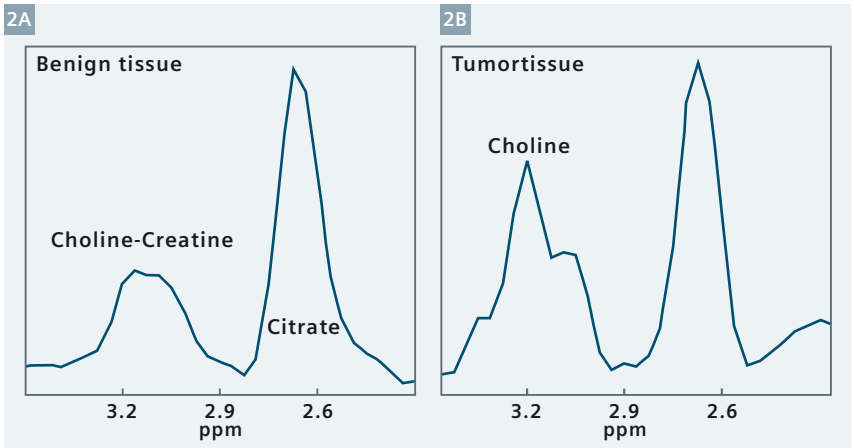

2 Examples of ^{1}H MRSI spectra acquired from benign prostate tissue and tumor at 1.5T.

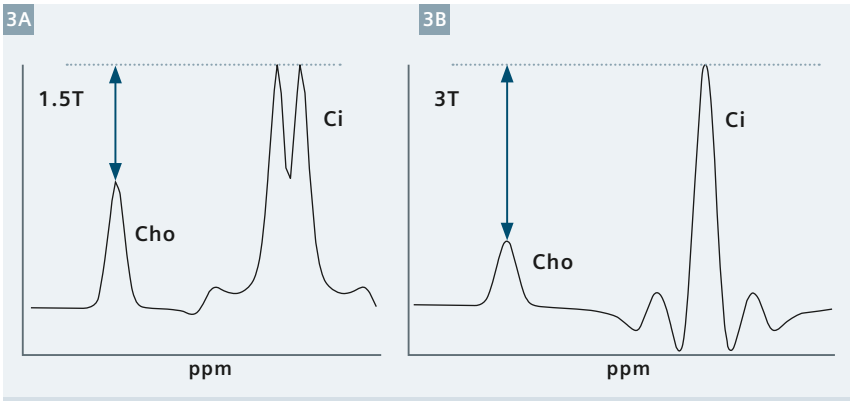

3 Simulated spectral shape of Cho and Ci for typical echo times (120 ms at 1.5T, 145 ms at 3T). Identical concentrations, i.e. scale factors, are applied, but different line broadening of the signals (4 Hz at 1.5T; 8 Hz at 3T). Note the difference in the spectral shape of Ci and the different peak amplitude ratios for Cho/Ci.

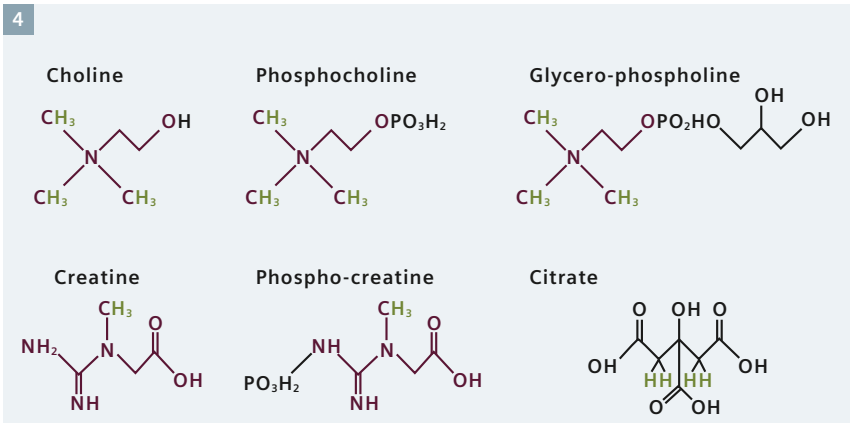

4 Structural formulas of the key small molecule metabolites observed in the spectra of prostate tissue. For each group, cholines and creatines, the common moiety is highlighted in red. The protons that give the MR spectral resonances present in the choline-creatine region are indicated in green. Choline-containing metabolites have 9 co-resonant protons in the region 3.2–3.25 ppm. Creatines have three co-resonant protons at 3.05 ppm. Citrate has four protons that resonate at two chemical shifts (2.6 and 2.7 ppm), one for each proton in a pair bonded to the same carbon. This pair also has a coupling between them and the symmetry of the whole molecule ensures that two protons co-resonate at each frequency.

part of prostatic fluid, which has a high concentration of this metabolite. Prostate carcinomas do not accumulate zinc ions, so they do not have this high citrate concentration. The increased presence of tumor cells within a ^{1}H MRSI voxel can, therefore, have two diminishing effects on the observed citrate signals: epithelial cells that accumulate citrate can transform into, or be replaced by, tumor which has low citrate, or the lesion can grow through the ductal spaces, thus displacing the prostatic fluid. The relative contribution of each of these two physiological changes, whether we are observing tumor formation and malignant progression or a histological change in tumor invasion of ductal structure, is not yet known. It is, however, clear that there is an inverse correlation of the levels of citrate metabolite and tumor cell density with some evidence to support a similar correlation with the aggressiveness of the tumor as well [8].

The introduction of a metabolite ratio

To transform the described changes in choline and citrate signals between benign (high citrate) and tumorous tissue (low citrate, high choline) into a marker for prostate cancer, the metabolite ratio was introduced [3-5]. The signal intensities of the different spectral peaks were quantified by simple integration of the two groups of resonances (the choline-creatine region and the citrate group), and the results were expressed as a ratio of the two. This gave the choline plus creatine over citrate ratio (abbreviated to CC/C [4]) or its inverse (with citrate as the numerator, [3, 5]). With choline in the numerator and citrate in the denominator, it became a positive biomarker for the presence of cancer.

Acquiring the MRSI data sets

As the prostate is embedded in lipid tissue, and lipids can cause very strong unwanted resonance artefacts in prostate spectra, the pulse sequence to acquire proton spectra is equipped with five properties to keep lipid signals out and retain optimal signals-of-interest in the whole prostate [9].

1. Localization of the signal with slice-selective pulses. The point resolved spectroscopy sequence (PRESS) is a combination of one slice selective excitation pulse and two slice selective refocusing pulses leading to an echo at the desired echo time. The three slices are orthogonal, producing an echo of the volume-of-interest (crossing of three slices) only.
2. Weighted acquisition and filtering. Proton MRSI data sets are acquired using a phase encoding technique where the gradients across spatial dimensions are varied with each repeat of the pulse sequence. By using weighted averaging of these phase encoding steps (smaller gradient steps are averaged more often than larger gradient steps) and adjusted filtering of the noise in these weighted steps, the resulting shape of a voxel after the mathematical translation of the signal into an image (Fourier Transform)

is a sphere. Contrary to conventional acquisition without filtering, the spherical voxels after filtering are not contaminated with signals from non-neighboring voxels.

3. Frequency-selective water and lipid suppression. The pulse sequence has two additional refocusing pulses that only touch upon water and lipid signals. Together with strong crushing gradients, signals from water and lipids are suppressed.
4. Outer volume suppression. Around the prostate, slice-selective pulses can be positioned to suppress all signals in the selected slabs. These slices can be positioned quite close to the prostate, even inside the PRESS-selected volume-of-interest.
5. Long echo time. To accommodate all localization and frequency selective pulses, the echo time of ^{1}H MRSI of the prostate is around 120 ms at 1.5T and 145 ms at 3T. At longer echo times, lipid signals decay due to their short T2 relaxation time.

The prostate is small enough (< 75 cubic centimetres) to allow a 3D ^{1}H MRSI data set to be acquired, with complete organ coverage, within 10 minutes of acquisition time. The nominal voxel size is usually around 6 × 6 × 6 mm, which after filtering as described above results in a true voxel size of 0.63 cm^{3}.

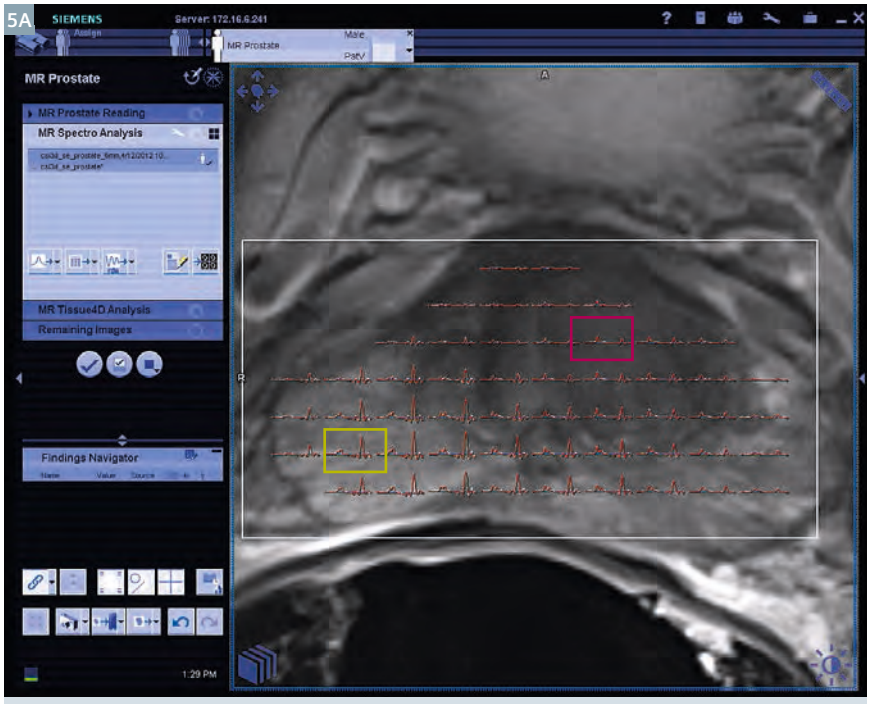

5 T2-weighted MRI image of a transverse section through a prostate as shown in figure 1 with an overlaid grid of MRSI-voxel data displayed as fitted spectra **(5A)**.

Spectral patterns

Due to multiple different protons in the molecule, a single metabolite can have multiple resonances. If interactions exist between protons within a metabolite, the shape of a spectral peak can be complicated. A resonance group of protons that has a mixture of positive and negative parts is said to have a dispersion component in its shape; a symmetrical-positive peak is referred to as an absorption shape. Choline and creatine resonances appear as simple peaks (singlets),

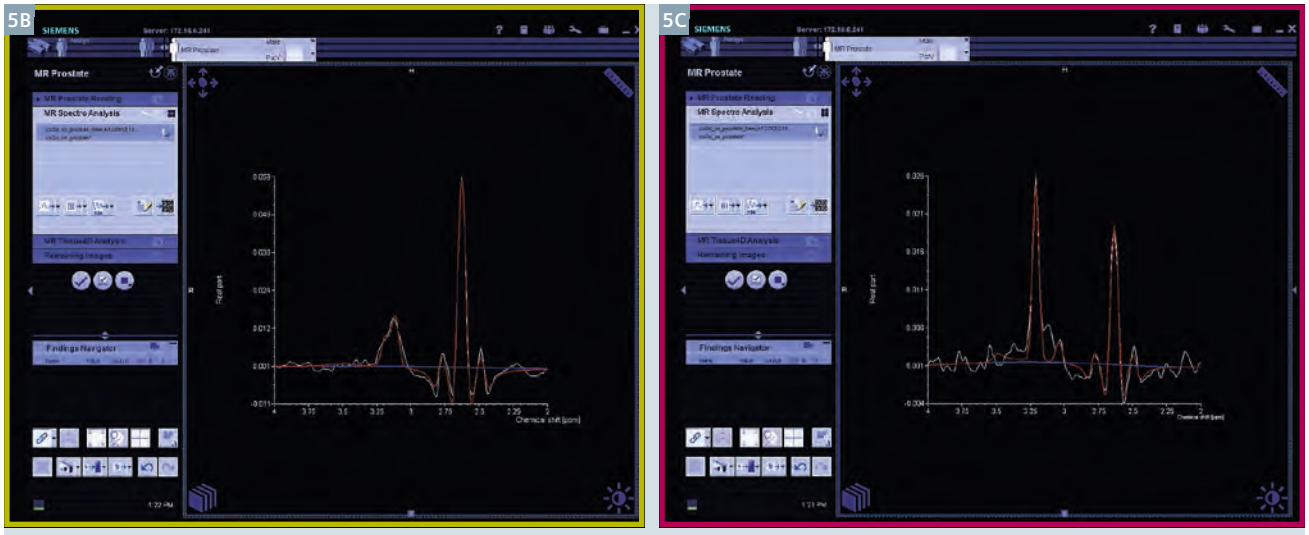

5 Two spectra (shown previously in figure 1) with their fitted model metabolite signals **(5B, C)**.

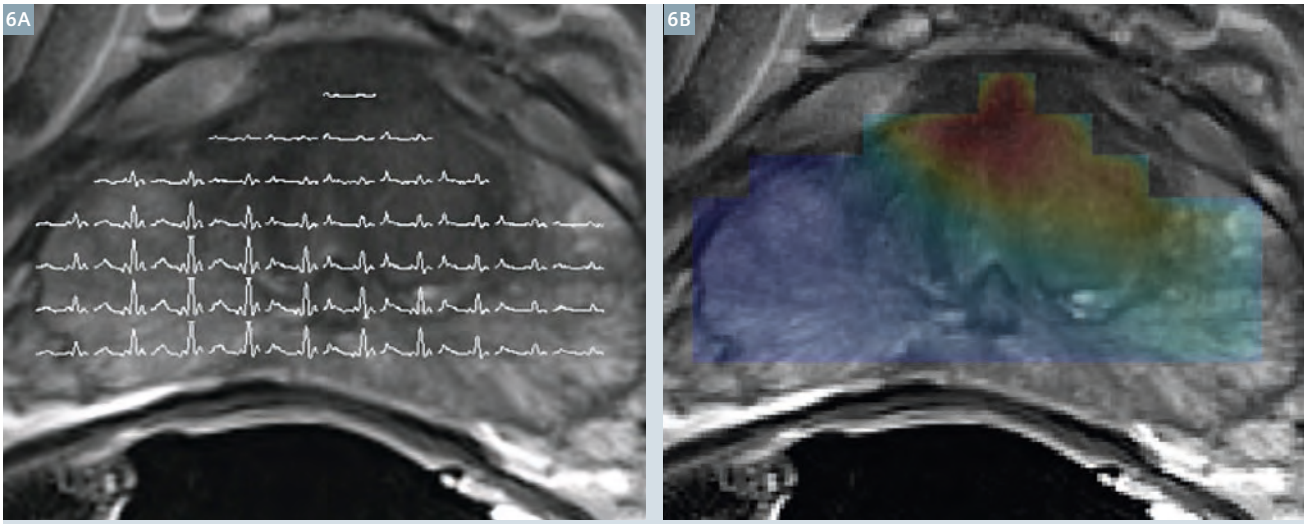

6 T2-weighted MR image of a transverse section through a prostate as shown in figure 1 with an overlaid grid of MRSI-voxel data displayed as spectra **(6A)** and as the pseudo integral CC/C ratio **(6B)** from metabolite fitting of the spectra. The ratio data points are interpolated and shown on a color scale of values from 0 (blue) to 3 (red). The tumor containing region of the prostate corresponds to the higher ratio values: the cyan-red area in the image.

although they very often cannot be separated from each other as they overlap within *in vivo* spectral linewidths. The structure of citrate, given in figure 4, results in protons at two different chemical shifts, with coupling between each proton and one other (a strongly coupled spin system). The spectral shape of these protons depends on their exact chemical shift, the coupling constant between them, the pulse sequence timing and the main magnetic field strength. At an echo time of 120 ms at 1.5T (and a very short delay between excitation and first 180 degree refocusing pulse), the spectral peaks of citrate are close to a positive absorption mode. The spectral shape consists mainly of an inner doublet with small side lobes on the outer wings. Together with line broadening the citrate protons quite closely resemble a single, somewhat broadened peak. The small side lobes around this peak are hardly detectable over the spectral noise *in vivo*. At 3T with an echo time of 145 ms (examples given in Fig. 1), the negative dispersion components of the citrate shape cannot be ignored. Its side lobes are substantially larger and reveal also some negative components [10]. Therefore the area under the curve, the integral, is substantially smaller at 3T than at 1.5T. Because of its complicated shape, it is essential at 3T to incorporate this shape in quantification of the signal.

Signal quantification by integration or metabolite fitting

The size of the peaks of the individual resonances represent the amount of the metabolite present in the voxel. Integration provides a simple method to quantify the spectra, as long as all signals have an absorption shape. Although it cannot discriminate between overlapping resonances, as long as overlapping signals (choline and creatine) are summed in a ratio this does not matter. With clear separation between citrate resonances and the choline-creatine region, the CC/C ratio can be calculated. However, as pointed out earlier, the spectral shape of citrate is not straightforward, and ignoring the small satellites at 1.5T, or simply integrating the large dispersion parts of the signal at 3T, would inevitably lead to underestimation of the total citrate signal intensity. An alternative is to fit the spectra with models of the citrate resonances with their expected shape. The shape can either be measured, using a solution of citrate placed in the MRI system and a spectrum acquired with the same sequence as the *in vivo* data, or it can be calculated using a quantum mechanical simulation (Fig. 3). By this process of spectral fitting, models of each metabolite's spectral peaks are fit to the total spectrum and the intensities of each fitted model are calculated. A linear combination of the metabolite models is found by the fitting routine such that

$$\text{Data} = C_1{}^{*}\text{choline model} + C_2{}^{*}\text{creatine model} + C_3{}^{*}\text{citrate model} + \text{baseline} \qquad \text{Eqn1.}$$

The coefficients $C_{1\text{-}4}$ give the relative concentrations of the individual metabolites.

When fitting with *syngo*.via, the result of a fit to a spectral peak can be expressed in two ways: as an integral value, which describes the area under the fitted spectral peak, or as a relative concentration (incorporating the number of protons in the corresponding peak) of the metabolite, called the scale factor (SF) of the metabolite.

As noted earlier, the integral value of citrate is different for 1.5 vs. 3 Tesla due to the different spectral patterns and would also change if pulse sequence timing other than standard

Table 1: Typical integral values of the CC/C ratio in prostate tissue at 1.5T [17] and pseudo integral values of CC/C at 3T [18]:

Tissue	1.5 Tesla*	3 Tesla**
Non-cancer peripheral zone	0.28 (0.21– 0.37)	0.22 (0.12)
Non-cancer central gland* **	0.36 (0.28–0.44)	0.34 (0.14)
Cancer	0.68 (0.43–1.35)	1.3 (3.7)

*median and 25th and 75th percentile **mean and standard deviation ***combined transition zone and central zone

would be used. If the scale factor is multiplied with the number of resonating protons (#H), it represents the intensity of a signal, in relation to the integral value of a pure singlet of one resonating proton in absorption mode. We call this entity pseudo integral, which is calculated as A.

pseudo integral (Metabolite) = #H * SF (Metabolite).

For citrate this pseudo integral is perhaps best described as the numerical integral of the magnitude (all negative intensity turned positive) of the citrate spectral shape, ignoring signal cancellations of absorption and dispersion parts of the shape.

The spectral fits are shown for the two spectra in figure 5 with model spectra of the three metabolites choline, creatine and citrate. It can be seen from these spectra that the relative amplitudes of the metabolites vary between the benign and the tumor spectrum. As expected, the benign spectrum has a higher citrate amplitude while the tumor has a greater choline amplitude, relative to the other metabolites. Combined in the CC/C ratio, the positive biomarker for the presence of tumor in the prostate is calculated.

Depending on the used quantification (spectral integration without fitting (a), fitted relative concentrations (b) or pseudo integrals (c)) the CC/C can be calculated by:

(a) {Integral(Choline) + Integral (Creatine)} / Integral(Citrate)

(b) {SF(Choline) + SF(Creatine) } / SF(Citrate)

(c) {9*SF(Choline) + 3*SF(Creatine)} / 4*SF(Citrate), respectively.

The numbers in the last equation correspond to the number of protons of the different signals. Generally, use of the pseudo integral ratio is strongly preferred, as it is least sensitive to large variations in individual metabolite fits in overlapping signals (choline and creatine). Note (again) that this pseudo integral ratio does not aim to provide a ratio of absolute metabolite concentrations, as this is very difficult with overlapping metabolite signals, partially saturated metabolite signals due to short TR (T1 effects), and variation in signal attenuation due to the use of a long echo time (T2 effects).

Now, what could be the effect on the ratio if further metabolites are included in the fitting? Could even polyamines be incorporated in the analysis [11]? After separate fitting, the main focus of the analysis could just be on choline and citrate, which have opposite changes in intensity with cancer, to make a simpler and potentially more sensitive choline/citrate ratio. Various metabolite ratios have been proposed [12, 13], and there is certainly value in using choline over creatine as a secondary marker of tumor malignancy that can give complementary information to the CC/C ratio [14-16]. However, any of these interpretations are limited by how well the individual metabolite resonances can be resolved. At 3T the choline, polyamines and creatine resonances all overlap (Figs. 1 and 5). In practice this lack of resolution in the spectrum translates to errors in the model fitting where one metabolite can be overestimated at the expense of another. For example a choline over citrate ratio could be underestimated if the polyamines fit was overestimated and accounted for some of the true choline signal. While acquisition and fitting methods are being actively researched to improve the individual quantification of these metabolites, it is more reliable to stick to the pseudo-integral CC/C ratio.

Once reliably calculated, the CC/C ratio combines the essence of the observable spectroscopic data into a single quantity that can be displayed on an image (Fig. 6), combining the key information into a simple to read form for radiological reporting.

Published values of the ratios for tumor and benign tissue, which are calculated in a similar way to the *syngo*.via fitting, are listed in table 1.

Future perspective of MRSI for prostate cancer

The CC/C ratio is the most used method for interpreting ^{1}H MRSI data of prostate and prostate cancer. It remains, essentially, the integral of the choline-creatine region divided by the citrate region, a simple combination of the metabolite information in a single-value marker that is sensitive to the presence of tumor. The use of areas under the resonances in the ratio has the implication that the absolute value of this biomarker is largely dependent on the acquisition sequence used. Any change in field strength, the pulses or pulse timings will change resonance amplitude and shape due to T1 and T2 relaxations and the scalar couplings of especially citrate. Values of the ratio quoted in the literature for tumor or benign tissues depend strongly on how the

ratio is actually calculated and are, therefore, often not directly comparable. However, using the Siemens-supplied default protocols for acquisition and *syngo*.via postprocessing enables one to make use of published values as given in table 1, and incorporate ^{1}H MRSI of the prostate into their clinical routine.

References

1 Siegel R, Naishadham D, Jemal A. Cancer statistics, 2012. CA Cancer J Clin 2012; 62(1):10-29.

2 Hoeks CMA, Barentsz JO, Hambrock T, Yakar D, Somford DM, Heijmink SWTPJ, Scheenen TWJ, Vos PC, Huisman H, van Oort IM, Witjes JA, Heerschap A, Fütterer JJ. Prostate Cancer: Multiparametric MR Imaging for Detection, Localization, and Staging. Radiology 2011; 261: 46 –66.

3 Heerschap A, Jager GJ, van der Graaf M, Barentsz JO, Ruijs SH. Proton MR spectroscopy of the normal human prostate with an endorectal coil and a double spin-echo pulse sequence. Magn Reson Med 1997;37(2):204-213.

4 Kurhanewicz J, Vigneron DB, Hricak H, Parivar F, Nelson SJ, Shinohara K, Carroll PR. Prostate cancer: metabolic response to cryosurgery as detected with 3D H-1 MR spectroscopic imaging. Radiology 1996;200(2):489-496.

5 Kurhanewicz J, Vigneron DB, Nelson SJ, Hricak H, MacDonald JM, Konety B, Narayan P. Citrate as an *in vivo* marker to discriminate prostate cancer from benign prostatic hyperplasia and normal prostate peripheral zone: detection via localized proton spectroscopy. Urology 1995;45(3):459-466.

6 Glunde K, Bhujwalla ZM, Ronen SM. Choline metabolism in malignant transformation. Nat Rev Cancer;11(12): 835-848.

7 Costello LC, Franklin RB. Novel role of zinc in the regulation of prostate citrate metabolism and its implications in prostate cancer. The Prostate 1998; 35(4):285-296.

8 Giskeodegard GF, Bertilsson H, Selnaes KM, Wright AJ, Bathen TF, Viset T, Halgunset J, Angelsen A, Gribbestad IS, Tessem MB. Spermine and citrate as metabolic biomarkers for assessing prostate cancer aggressiveness. PloS one;8(4):e62375.

9 Scheenen TW, Klomp DW, Roll SA, Futterer JJ, Barentsz JO, Heerschap A. Fast acquisition-weighted three-dimensional proton MR spectroscopic imaging of the human prostate. Magn Reson Med 2004;52(1):80-88.

10 Scheenen TW, Gambarota G, Weiland E, Klomp DW, Futterer JJ, Barentsz JO, Heerschap A. Optimal timing for *in vivo* ^{1}H-MR spectroscopic imaging of the human prostate at 3T. Magn Reson Med 2005;53(6):1268-1274.

11 Shukla-Dave A, Hricak H, Moskowitz C, Ishill N, Akin O, Kuroiwa K, Spector J, Kumar M, Reuter VE, Koutcher JA, Zakian KL. Detection of prostate cancer with MR spectroscopic imaging: an expanded paradigm incorporating polyamines. Radiology 2007;245(2):499-506.

12 Garcia-Martin ML, Adrados M, Ortega MP, Fernandez Gonzalez I, Lopez-Larrubia P, Viano J, Garcia-Segura JM. Quantitative (1) H MR spectroscopic imaging of the prostate gland using LCModel and a dedicated basis-set: correlation with histologic findings. Magn Reson Med; 65(2):329-339.

13 Heerschap A, Jager GJ, van der Graaf M, Barentsz JO, de la Rosette JJ, Oosterhof GO, Ruijter ET, Ruijs SH. *In vivo* proton MR spectroscopy reveals altered metabolite content in malignant prostate tissue. Anticancer research 1997; 17(3A): 1455-1460.

14 Jung JA, Coakley FV, Vigneron DB, Swanson MG, Qayyum A, Weinberg V, Jones KD, Carroll PR, Kurhanewicz J. Prostate depiction at endorectal MR spectroscopic imaging: investigation of a standardized evaluation system. Radiology 2004;233(3):701-708.

15 Futterer JJ, Scheenen TW, Heijmink SW, Huisman HJ, Hulsbergen-Van de Kaa CA, Witjes JA, Heerschap A, Barentsz JO. Standardized threshold approach using three-dimensional proton magnetic resonance spectroscopic imaging in prostate cancer localization of the entire prostate. Investigative radiology 2007;42(2):116-122.

16 Kobus T, Hambrock T, Hulsbergen-van de Kaa CA, Wright AJ, Barentsz JO, Heerschap A, Scheenen TW. *In vivo* assessment of prostate cancer aggressiveness using magnetic resonance spectroscopic imaging at 3 T with an endorectal coil. European urology;60(5):1074-1080.

17 Scheenen TWJ, Fütterer J, Weiland E and others. Discriminating cancer from noncancer tissue in the prostate by 3-dimensional proton magnetic resonance spectroscopic imaging: A prospective multicenter validation study. Invest Radiol 2011;46(1):25-33.

18 Scheenen TW, Heijmink SW, Roell SA, Hulsbergen-Van de Kaa CA, Knipscheer BC, Witjes JA, Barentsz JO, Heerschap A. Three-dimensional proton MR spectroscopy of human prostate at 3 T without endorectal coil: feasibility. Radiology 2007;245(2):507-516.

19 Kobus T, Wright AJ, Scheenen TW, Heerschap A. Mapping of prostate cancer by ^{1}H MRSI. NMR Biomed. 2013 Jun 13. doi: 10.1002/nbm.2973. [Epub ahead of print] PMID:23761200.

Contact

Tom Scheenen, Ph.D.
Radboud University Nijmegen
Medical Centre
Radiology Department
P.O. Box 9102
6500 HC Nijmegen
The Netherlands
Tom.Scheenen@radboudumc.nl


Alan Wright


Arend Heerschap


Thiele Kobus


Tom Scheenen